Full broadband processing including total Q compensation in the presence of gas

Barry Hung[1], Xusong Wang[1], Ying Peng Phan[1], Riaz Alai[2], Kefeng Xin[1], Yi He[1], Nurul Nadzirah Rahman[2] and Wai Hoong Tang[2]
[1]CGG, [2]PETRONAS Carigali Sdn. Bhd

Summary

Recent efforts in marine broadband processing have largely been focused on source and receiver deghosting. To fully recover the frequency bandwidth of seismic data, the anelastic nature of the earth needs to be taken into account. In addition, in the presence of gas anomalies, attenuation of seismic waves will cause further degradation in the resolution of migrated images. By quantifying the attenuation of seismic energy using quality factor Q, we can model the intrinsic absorptive nature of the earth as background Q and the localized absorptive bodies, e.g. gas pockets, as anomalous Q. Using the frequency information and the amplitude information of the data to estimate the background Q (FS-QTomo) and anomalous Q (A-QTomo), respectively, the attenuation effects of the earth can be compensated by the application of Q-PSDM in the presence of gas with the resultant combined Q model. The accuracy of these processes is further enhanced by broadband processing with deghosting in terms of better estimation of the centroid frequency for FS-QTomo and deeper penetration of low frequency signal through the gas bodies for A-QTomo. Thus, the interplay of deghosting and Q tomography provides a full broadband processing workflow for restoring the distortion of amplitude, frequency and phase caused by the combined effects of the earth's anelasticity and gas pockets. We applied our workflow on a field data example and demonstrated through this first case study that high resolution broadband seismic data with improved signal to noise ratio (S/N) can be obtained.

Introduction

Extending the usable frequency through broadband acquisition and processing has proven to be beneficial in the application of FWI (Ratcliffe *et al.*, 2013), the enhancement of imaging (Zhou *et al.*, 2014), studies of inversion (Soubaras *et al.*, 2012), etc. In the area of broadband processing, one of the key steps is deghosting. In recent years active research has been conducted into both pre-migration and post-migration deghosting algorithms, as well as its application to different marine acquisition configurations, e.g. conventional shallow cable, variable-depth cable, multi-component cable etc.. For full broadband processing, however, the attenuation effects of the earth's subsurface need to be taken into account. To this end, the intrinsic anelastic nature of the earth must be considered in the processing workflow. Moreover, in the presence of gas, both as shallow pockets and as commercial reservoirs (not an uncommon geological setting in many parts of the world), localized strong absorption from these gas bodies will cause amplitude dimming and frequency dependent dissipation, and this degradation in signal needs to be recovered.

Quantifying the attenuation of seismic energy due to the earth's anelasticity as background Q (Q_b) and gas bodies as anomalous Q (Q_a), we have proposed two separate methods for estimating: (1) Q_b using frequency shift Q tomography (FS-QTomo, Xin *et al.*, 2014) that adaptively extracts dissipation time information from the change of spectral features of the seismic data and (2) Q_a using amplitude Q tomography (A-QTomo, Xin and Hung, 2011) that makes use of the amplitude ratio between affected and unaffected areas for tomographic inversion to obtain the Q field due to gas. However, the practical application of the combined Q models has not yet been shown. Furthermore, the interplay between deghosting and FS-QTomo and A-QTomo has not been explored, namely, (1) the estimation of frequency shift will be more accurate with deghosted data for FS-QTomo and (2) the deeper penetration of extended low frequencies from deghosted data allows more energy to pass through gas bodies thereby helping the amplitude ratio estimation in A-QTomo.

In this paper, we propose a broadband processing workflow that is purely data driven and applicable to both conventional towed and variable depth towed marine streamer data. Three important ingredients of our workflow are highlighted: (1) deghosting; (2) FS-QTomo and A-QTomo; (3) prestack depth Q migration (Q-PSDM). We first demonstrate through a simple synthetic example how FS-QTomo can benefit from the removal of source and receiver notches in obtaining more accurate Q field. We then utilize a field data example from offshore Malaysia that exhibits severe absorption resulting from gas pockets to show how our workflow can provide high resolution delineation of the target structures and reveal the gas leaking features from the deep reservoir.

Benefits of deghosting for Q Tomography

Figure 1 shows our simplified proposed workflow for full broadband processing in the presence of gas with only the key steps being specified. Since the topic of broadband processing includes a wide range of practices, we limit the scope of this paper by focusing on the highlighted boxes in the figure. In practice, iterations may be needed in updating Q fields and velocity consecutively; here we depict a linear approach for the sake of simplicity.

DOI http://dx.doi.org/10.1190/segam2015-5936968.1

Regarding the influence of deghosting on Q tomography, for the component of Q_a, it has been demonstrated recently that, in the presence of gas anomalies, the extension of usable low frequencies resulting from receiver deghosting enables faster convergence of A-QTomo (Zhou *et al.*, 2013). For the component of Q_b, however, it has not been discussed how deghosting can benefit its estimation. Following our approach of using the shift in the centroid frequency measured at the source and receiver locations for estimating Q_b with FS-QTomo (Xin *et al.*, 2014), we generated a simple synthetic example with different interval Q values as shown in Figure 2 to illustrate the importance of ghost free data for FS-QTomo in estimating the Q_b. The seismic data depicted in Figure 2 are obtained by performing visco-acoustic wave equation modeling using a Ricker wavelet of 30 Hz with Figure 2b and 2c displaying the seismic responses of the first event with and without source and receiver ghosts (both source and receiver depths are at 15 m), respectively. Figure 2d displays the amplitude spectra of the two wavelets. With the application of FS-QTomo, we obtained the Q_b models as plotted in Figure 2e. It can be seen that the Q_b values obtained from ghost free wavelet are very close to the correct values but those obtained from wavelet with ghost have a discrepancy ranging from 6% to 16% in this case. This verifies the importance of deghosting for Q_b estimation using the centroid frequency shift method. Thus, for broadband processing, it is necessary to include deghosting for Q tomography.

Example

We applied the workflow stated in Figure 1 on flat towed marine data (source and streamer depth are at 5 m and 6 m, respectively) acquired offshore Malaysia. Figure 3 displays a stacked PSDM section of previously processed data where the presence of extended carbonate structures act as significant absorptive layers which degrades the resolution of the events underneath making them difficult to delineate and interpret (Alai *et al.*, 2014). In addition, the gas pockets, indicated by the dashed ellipse, distort the signals near the top of the carbonates in such a way that the event becomes discontinuous as a result of amplitude dimming and phase distortion caused by the gas bodies.

As shown in Figure 4, source and receiver ghosts were effectively removed by applying pre-migration deghosting based on the bootstrap approach (Wang *et al.*, 2013),. The magnified sections verify the preservation of primary events after deghosting. After performing multiple attenuation and PSDM on the deghosted data, we obtained a migrated seismic section as depicted in Figure 5. Compared with the PSDM result without deghosting shown in Figure 2, the enhancement of low frequency response allows the deeper part of the data to be imaged with higher S/N. The next step is to handle the effects caused by the gas pockets. By applying our A-QTomo on the common image gathers (CIGs) using amplitude ratio information measured from picked horizons underneath the gas bodies, we obtained an inverse Q_a (1/ Q_a) field as shown in Figure 6. Applying Q-PSDM (Xie *et al*., 2009) using this Q field, we generated a seismic section as displayed in Figure 7. It can be seen that the distortion in amplitude and phase of the events in the affected area has been nicely compensated. Besides enhancing the continuity of the top of the carbonates as indicated by the arrows, the processes of A-QTomo and Q-PSDM also help in revealing the gas leaking feature, as indicated by the dotted circle, which has not been identified before.

Nevertheless, to further enhance the interpretability of the target events below the top of the carbonates, the background effect of attenuation needs to be addressed. From the Q-PSDM compensated gathers, we applied FS-QTomo on the data by picking events from CIGs, converting the picked events to time domain by applying reverse normal moveout, measuring the centroid frequency of the events in data domain and then estimating the Q_b model through tomographic inversion. Figure 8 shows the summation of inverse Q_b field and the inverse Q_a field. It can be observed that the distribution of Q_b is fairly consistent with the geological structures. This is also consistent with our observation of the application of FS-QTomo on another survey (Zhou *et al.*, 2014). Nevertheless, we have not previously presented a method for handling the combined effects due to Q_a and Q_b. In this example, we follow the approach used by Aki and Richards (1980) for obtaining the total Q, Q_{total}, by summing the inverse values of Q_a and Q_b:

$$\frac{1}{Q_{\text{total}}} = \frac{1}{Q_{\text{a}}} + \frac{1}{Q_{\text{b}}} \qquad (1)$$

The computed total Q field is plotted in Figure 8. Figure 9 displays the image after applying Q-PSDM using the Q_{total} volume. In comparison with the migrated result without Q compensation, the resolution of the events is much higher. In particular, the magnified sections of the carbonate layers clearly show the benefit of total Q compensation for better delineating the target structures making it easier for inversion work. The uplift is further confirmed by the comparison of the amplitude spectra in Figure 10. The stepwise widening of the frequency bandwidth is evident from the application of deghosting and total Q compensation. The step change in imaging between Figures 3 and 9 verifies the effectiveness of our workflow.

Conclusions

We have presented a broadband processing workflow that incorporates source and receiver deghosting with Q tomography and Q-PSDM in compensating the loss of

DOI http://dx.doi.org/10.1190/segam2015-5936968.1

signal due to ghost and the earth's absorption. We have shown the interplay between deghosting and Q tomography in enhancing the estimation of background Q and anomalous Q. We have successfully demonstrated the first application of combining the two Q models in a data-driven manner in compensating for the frequency dependent absorption on a flat-towed streamer survey.

Acknowledgements

The authors would like to thank PETRONAS Carigali Sdn. Bhd. for the permission of showing the results. Many thanks to PETRONAS project team : Dr. Mirza Arshad Beg, Mr. Zhu Jidong, Mr. Hairul Hafez Abu Bakar, Mr. Mohd Al-Amin B. Abd Mutalib, Mr. Ahmad Izzuddin B Yusof and Ms. Nurul Amira Bt Zulkurnain, and CGG for the permission to publish this work.

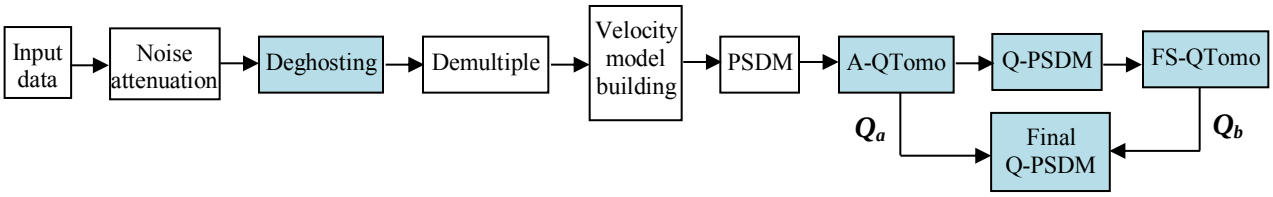

Figure 1: Proposed full broadband processing workflow in this paper.

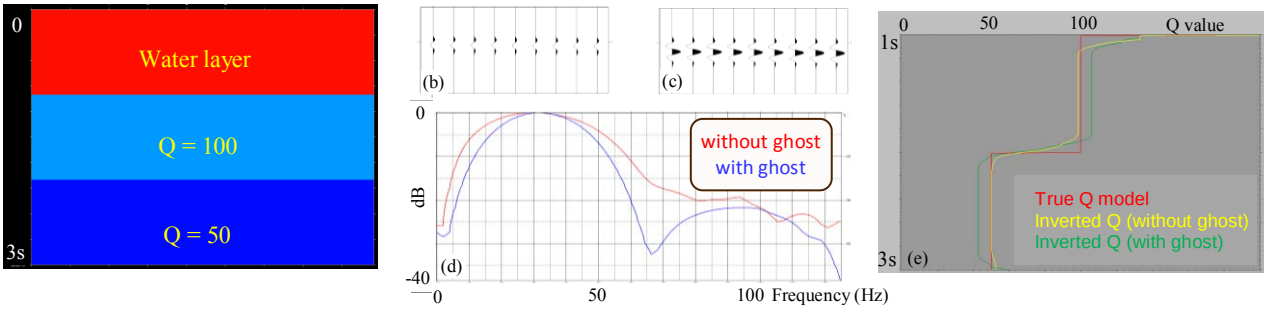

Figure 2: (a) Synthetic model with different interval Q values; (b) Modelled first event without ghost; (c) Modelled first event with ghost; (d) Amplitude spectra of the two wavelets; (e) Estimated Q values by FS-QTomo.

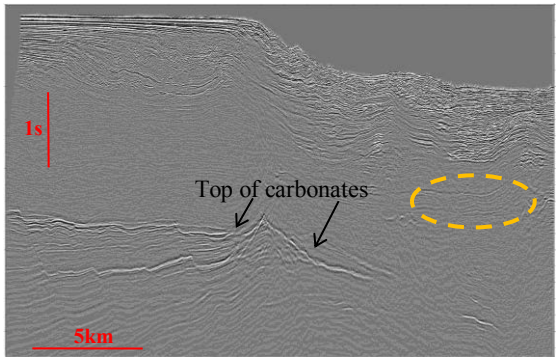

Figure 3: PSDM result from previous processing without deghosting and Q compensation. The data quality issue is highlighted by the presence of gas pockets (dotted circle) and lack of energy passing through the carbonates.

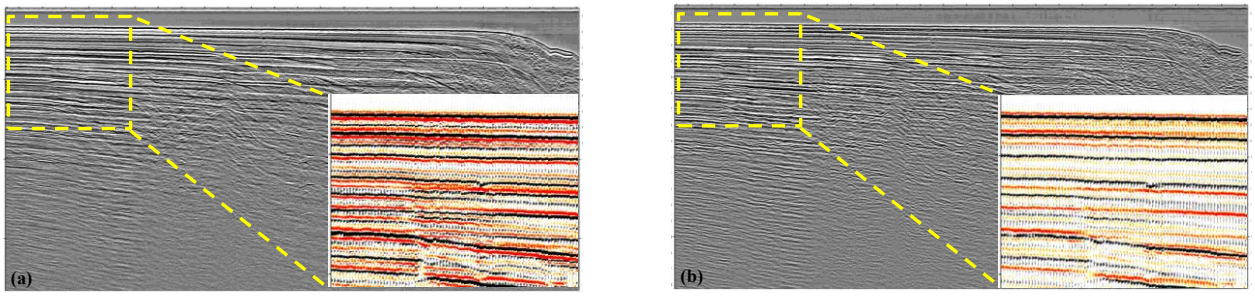

Figure 4: Common offset sections. (a) Before deghosting. (b) After deghosting.

DOI http://dx.doi.org/10.1190/segam2015-5936968.1

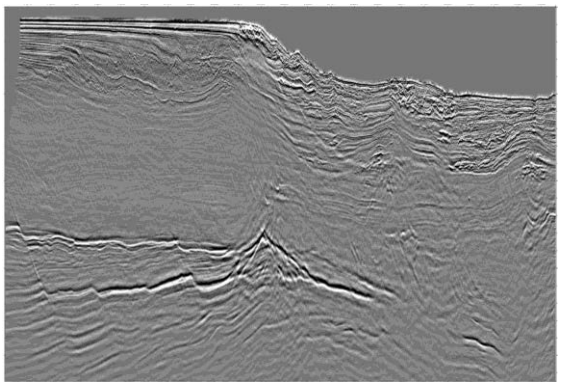

Figure 5: PSDM result with deghosting.

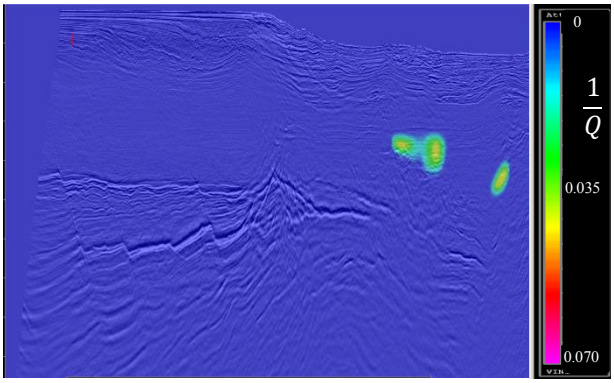

Figure 6: Inverse Q_a ($1/Q_a$) field obtained from A-QTomo.

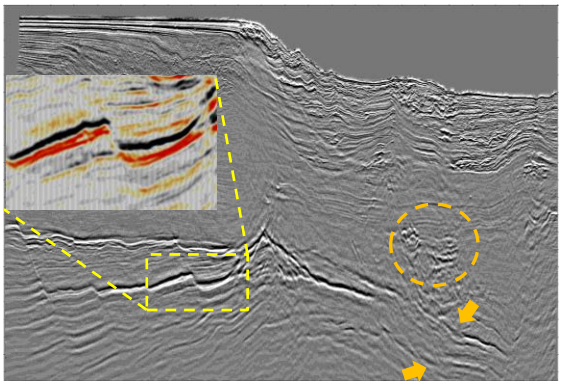

Figure 7: Q-PSDM result with deghosting and anomalous Q compensation. The events (indicated by the dotted circle and arrows) underneath the gas pockets are nicely restored.

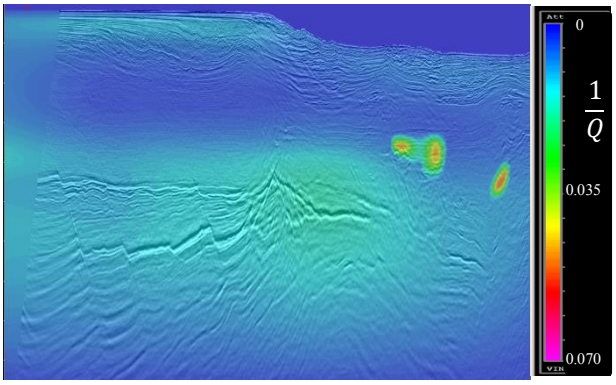

Figure 8: Inverse total Q ($1/Q_{total}$) field – summation of $1/Q_a$ and $1/Q_b$.

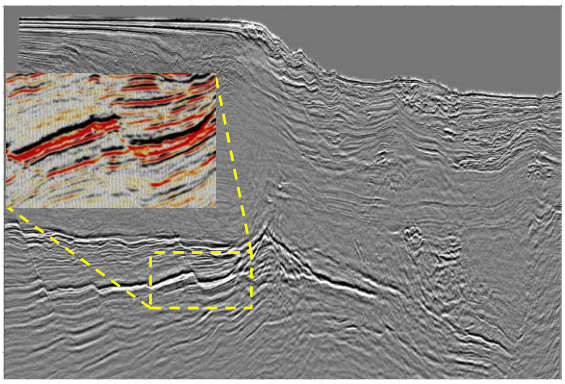

Figure 9: Q-PSDM result with deghosting and total Q compensation. The magnified section highlights the enhancement in resolution in comparison with the corresponding section in Figure 7.

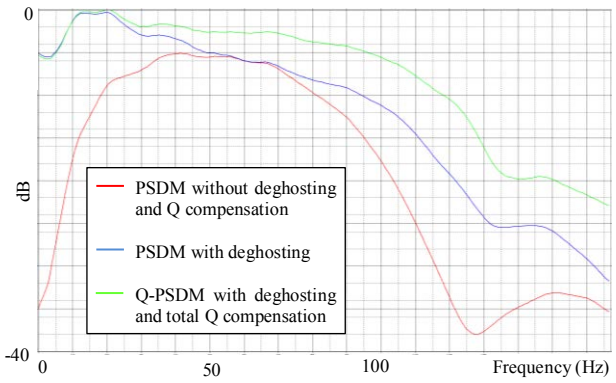

Figure 10: Amplitude Spectra. Stepwise extension of frequency bandwidth is observed with the application of deghosting and total Q compensation via Q-PSDM.

DOI http://dx.doi.org/10.1190/segam2015-5936968.1

EDITED REFERENCES

Note: This reference list is a copyedited version of the reference list submitted by the author. Reference lists for the 2015 SEG Technical Program Expanded Abstracts have been copyedited so that references provided with the online metadata for each paper will achieve a high degree of linking to cited sources that appear on the Web.

REFERENCES

Aki, K., and P. G. Richards, 1980, Quantitative seismology: Theory and methods: W. H. Freeman & Co.

Alai, R., N. N. Rahman, M. A.-A. B. Abd Mutalib, H. H. Abu Bakar, M. A. Beg, Y. P. Phan, and X. S. Wang, 2014, Re-acquiring or re-processing seismic data? A successful re-processing case study offshore Malaysia: 84th Annual International Meeting, SEG, Expanded Abstracts, 4325–4329.

Ratcliffe, A., R. Jupp, R. Wombell, G. Body, V. Durussel, A. Fernandes, B. Gosling, and M. Lombardi, 2013, Full-waveform inversion of variable-depth streamer data: An application to shallow channel modeling in the North Sea: The Leading Edge, **32**, 1110–1115, http://dx.doi.org/10.1190/tle32091110.1.

Soubaras, R., R. Dowle, and R. Sablon, 2012, BroadSeis: Enhancing interpretation and inversion with broadband marine seismic: CSEG Recorder, **37**, no. 7, 40–46.

Xie, Y., K. F. Xin, J. Sun, C. Notfors, A. K. Biswal, and M. K. Balasubramaniam, 2009, 3D prestack depth migration with compensation for frequency dependent absorption and dispersion: 79th Annual International Meeting, SEG, Expanded Abstracts, 2919–2923.

Xin, K. F., Y. He, Y. Xie, W.-Q. Xu, and M. Wang, 2014, Robust Q tomographic inversion through adaptive extraction of spectral features: 84th Annual International Meeting, SEG, Expanded Abstracts, 3726–3730.

Xin, K. F., and B. Hung, 2010, 3-D tomographic Q inversion for compensating frequency dependent attenuation and dispersion: 79th Annual International Meeting, SEG, Expanded Abstracts, 4014–4018.

Zhou, J., J. Y. Li, H. Ng, S. Birdus, K. H. Teng, Y. P. Phan, J. Sun, Y. He, and P. Chia, 2014, Unlocking the full potential of broadband data with advanced processing and imaging technology, a case study from NWS Australia: 84th Annual International Meeting, SEG, Expanded Abstracts, 3689–3693.

Zhou, J., X. D. Wu, K. H. Teng, Y. Xie, F. Lefeuvre, I. Anstey, and L. Sirgue, 2013, FWI-guided Q tomography and Q-PSDM for imaging in the presence of complex gas clouds, a case study from offshore Malaysia: 83rd Annual International Meeting, SEG, Expanded Abstracts, 4765–4769.

DOI http://dx.doi.org/10.1190/segam2015-5936968.1